PUBLISHED VERSION

http://hdl.handle.net/2440/78357

A Realistic Assessment of Recoverable Thermal Energy from Australian Geothermal Reservoirs: A Simulation Study

Nima Gholizadeh Doonechaly[1], Sheik S. Rahman[1] and Andrei Kotousov[2]

[1]School of Petroleum Engineering, University of New South Wales, Sydney, Australia, [2]School of Mechanical Engineering, University of Adelaide, Adelaide, Australia,

sheik.rahman@unsw.edu.au

Keywords: Reservoir stimulation, shear dilation, distributed dislocation, local thermal non-equilibrium, FEM.

Summary

This paper presents an innovative distributed dislocation theory for estimation of change in fracture aperture due fluid induced pressure. The new approach is used to analyze the potential for thermal energy recovery from the Patchawarra geothermal reservoir in Australia. Results of this study show that the time required to stimulate a 500 m2 reservoir rock and sustain commercial flow rate (80 l/s) is much greater (two to three folds) than that previously studied. These results, however, agree well with the experience of existing EGS trials around the world. Thermal stresses induced during the circulation of cold water have a significant bearing on the long term production rate. As thermal drawdown of the rock matrix takes place, tensile thermal stresses are induced which allow residing fractures to dilate and enhance permeability. This gradually increases the fluid velocities between the injector and producer, yielding increasing production rates with time. It was also observed that the maximum thermal energy that can be recovered by use of our current know-how would be as much as 42%.

Introduction

Stimulation of geothermal reservoirs by fluid induced shear displacement has been used to create Enhanced Geothermal Systems (EGS). Models used to predict the change in fracture aperture and the consequent permeability enhancement are based on simple laboratory tests and field observations as well as best-guess estimates. In this study the reservoir, wellbores and the natural fractures (discrete) are coupled in a poro-thermo-elastic environment. The distributed dislocation technique is used to simulate the roughness induced opening of fractures in the presence of compressive and shear stresses as well as fluid pressure inside the fracture. This technique has allowed us for the first time to compute accurately changes of aperture along the fracture length of any number of discrete fractures in all parts of the reservoir due to induced fluid pressure and temperature. We have used local thermal non-equilibrium due to circulation of cold fluid to account for long term response. Also considered are the characteristic properties of rock and fracture to accurately simulate rock deformation.

Model Setup

A square region of the Patchawarra geothermal reservoir is chosen with a side length of 500 m at a depth of 2660 m. The characteristic data for this reservoir is presented in Table 1. Two wells, injection and production are placed at a distance of 700m apart. The reservoir is divided into 140,000 grid blocks. Maximum and minimum horizontal principal stresses are acting along the x and y axis. Stress, rock and reservoir parameters used for this study is shown in Table 2.

Table 1: Characteristic data using STAR resistivity image logs from Well A.

Top	2660
Bottom	2879
Number of fractures	69
Dip	30-60
Azimuth	065°N
Azimuth STD	17°
Vertical Stress (MPa)	54
Max. Horizontal Stress (MPa)	79
Min. Horizontal Stress (MPa)	60

The abovementioned model is meshed using triangular elements. For improving the stability linear triangles are used for pressure and temperature and quadratic triangular element for the displacement degrees of freedom. No flow boundary condition is applied at the boundary of the reservoir and the fluid is injected at the injection well. The production well starts producing with a set pressure at the end of stimulation period.

Overall, four major models are integrated to estimate stress changes due to fluid induced pressure and thermal drawdown by circulation of cold fluid and consequent changes in permeability. They include: generation of subsurface fracture map, simulation of fluid flow and heat transfer and reservoir stimulation in poro-thermo-elastic environment.

Table2: Stress and reservoir data for Patchawarra formation geothermal reservoir.

Rock Properties	
Young's modulus (GPa)	56
Poisson's ratio	0.25
Density (kg/m^3)	2650
Fracture basic friction angle (deg)	40
Shear dilation angle (deg)	2.8
90% closure stress (MPa)	20
In situ mean permeability (m^2)	9.0 x 10^{-17}
Fracture properties	
Fractal Dimension, D	1.2
Fracture density (m^2/m^3)	0.33
Smallest fracture radius (m)	15
Largest fracture radius (m)	250
Stress data	
Maximum horizontal stress (MPa)	78.9
Minimum horizontal stress (MPa)	53.3

Fluid properties	
Density (kg/m^3)	1000
Viscosity (Pa s)	3×10^{-4}
Hydrostatic fluid pressure (MPa)	27.5
Injector pressure, stimulation (MPa)	51.7
Injector pressure, production (MPa)	32.6
Producer pressure, stimulation (MPa)	N/A
Producer pressure, production (MPa)	22.3
Other reservoir data	
Well radius (m)	0.1
Number of injection wells	1
Number of production wells	1
Reservoir depth (m)	2660

Generation of subsurface fracture map

A hybrid of deterministic and stochastic techniques is used to generate subsurface discrete fracture network (Gholizadeh Doonechaly and Rahman, 2012). In this study, the tectonic history and characteristic data on fracture properties as well as reservoir structure of the Patchawarra formation available in the open literature are used to construct the fracture map (Mildren and Burgess, 2005, see Table1).

For the purpose of modelling tectonic history and in-situ stress (current) a Finite Element Method (FEM) is used. The reservoir structure is reconstructed by unfolding and folding (reverse and forward model) in a single tectonic event. Also a non-linear visco-elastic model is used to consider the effect of deformation on rock viscosity. After reconstructing the original shape of the layer, stress tensor values as well as the stress invariants are calculated for each node based on the deformation history of the model. Mohr-Colomb fracture criterion, which relates the critical strength of the material to its stress state, is used to determine whether the obtained stress exceeds strength (shear) of the rock. If the obtained stress tensor satisfies failure criterion, stress invariants are used to calculate the rate of formation of fractures for each node. Rate of formation of fractures is used as one of the most important input parameters for the next step of the Neural-stochastic simulation. As part of neuro-stochastic simulation, fracture properties (fracture density and fractal dimension) are generated based on their characterized statistical distribution obtained from tectonic simulation and field data (as listed in Table 1). In the next step the reservoir is divided into a number of grid blocks. Fracture density and fractal dimension are estimated for the blocks where the fracture data are available. Then the neural network is used to develop a 3D continuum map of fracture density and fractal dimension. Finally, the sequential Gaussian stochastic simulation combined with simulated annealing technique is used to generate the discrete fracture network. The 2D discrete Fracture map of Patchawarra reservoir at depth of 2660m is presented in Fig.1.
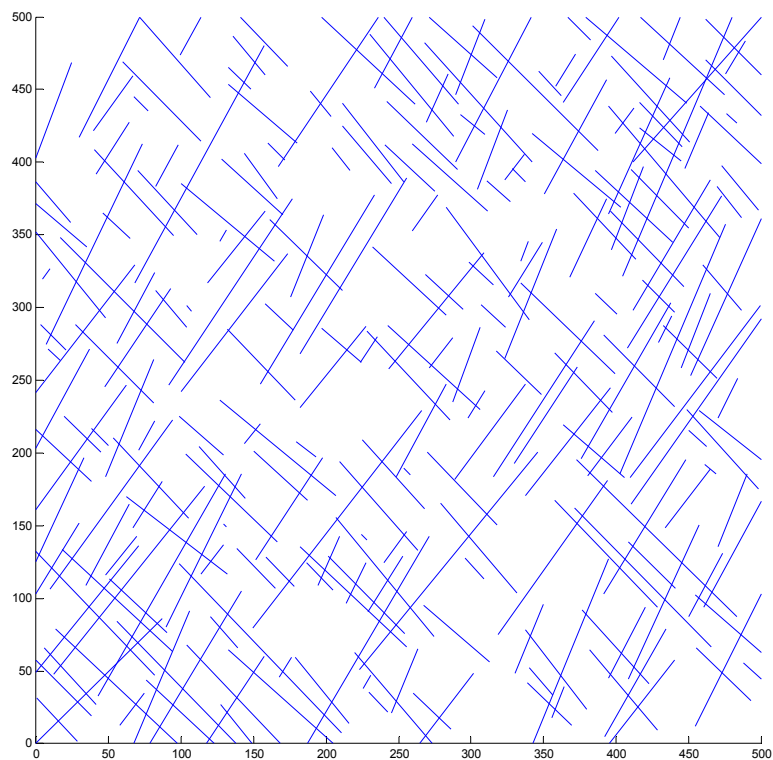
Figure 1: Patchawarra natural fracture network trace at 2660 m.

Fluid Flow Simulation

Fluid flow simulation is carried out using a hybrid of equivalent single continuum and discrete fracture approaches. For the single continuum approach, permeability tensor of each grid block is made known as a priori for the fractures shorter than 120 m. In this study, the effective permeability tensors as proposed by Teimoori and Rahman et al (2003) and later modified by Fahad and Rahman (2011) is estimated for each grid block. In this methodology, short fractures (less than 10m) are considered as part of the matrix pores and the fluid flow through them is simulated using the Darcy's law and Laplace equation. Also the boundaries of the short fractures are subjected to the interface boundary condition. Flow in the medium fractures (less than 120m) is characterized by the Cubic law. Flow region between matrix and fracture is characterized as Poisson's region and fluid flow in this region is simulated after Teimoori and Rahman, et al (2005). The effective permeability tensors are used in the next step as part of the thermo-poroelastic model of the reservoir. A representative schematic of the calculated grid based permeability tensor is shown in Fig. 2a.

In Fig 2b long fractures (longer than 120 m) are superimposed on effective permeability tensors calculated for medium to short fractures (less than 120m). Fluid flow is simulated using both effective permeability tensors and flow through discrete fractures as shown in Fig. 2b. Fractures bigger than 120 m, are discretized in the domain using zero thickness elements as shown in Fig. 3.

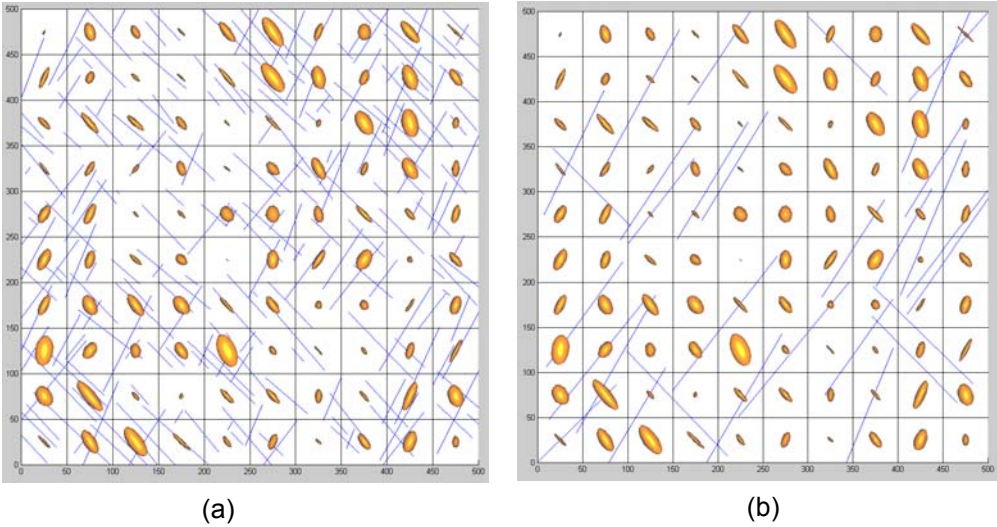(a)   (b)

Figure 2: (a) Natural fractures (shorter than 120 m) along with calculated permeability tensors for each grid block of 500 m x 500 m reservoir; (b) long fractures (longer than 120 m) superimposed on effective permeability tensors calculated for medium to short fractures (less than 120m)
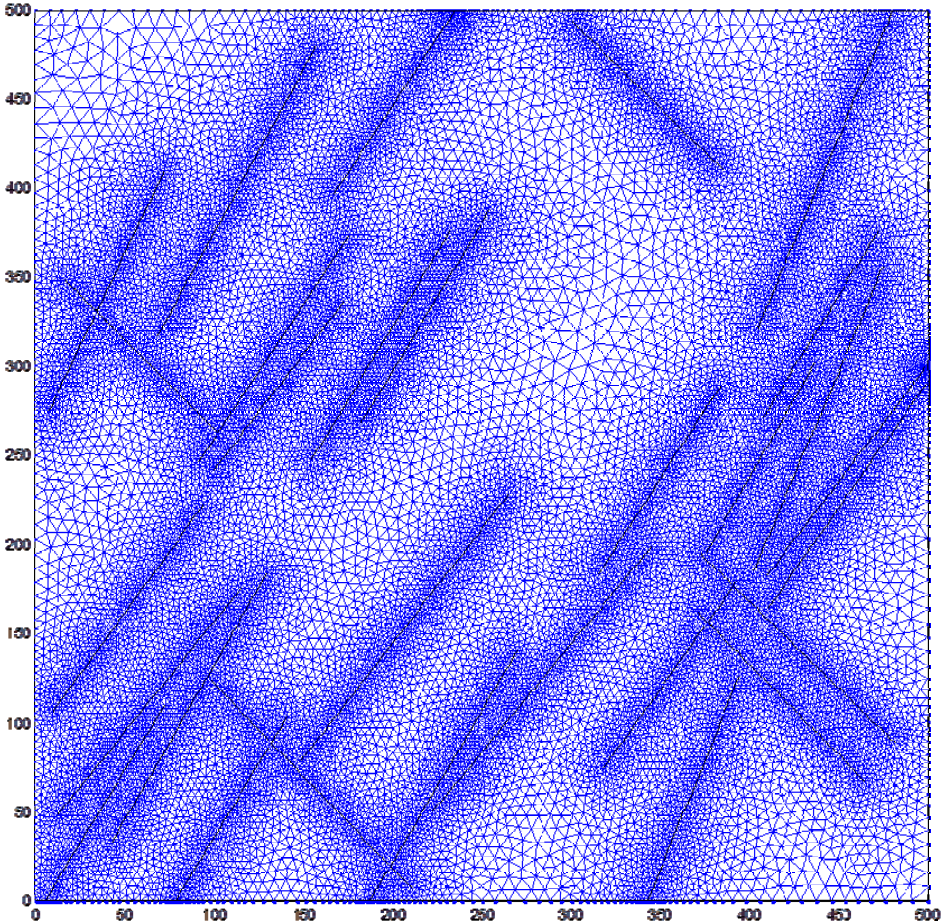

Figure 3: Discretisation of fractures longer than 120m

Heat transfer model

A finite element based thermo-poroelastic model is developed for evaluating fluid flow, pressure and temperature at different sections of the reservoir. The het transfer model consists of three parts: a) deformation of the porous media within the reservoir caused by the in-situ stresses and injection pressure, b) fluid flow within the reservoir, and c) thermal conduction and convection by diffusion and advection respectively. The governing equations used for the fully coupled thermo-poroelasticity are as follows: (Kurashige, 1989; Ghassemi et al., 2002; Shaik and Rahman, 2011):

$$\left(K + \frac{G}{3}\right)\nabla(\nabla \cdot u) + G\nabla^2 u - \alpha\nabla p - \gamma_1 \nabla T_R = 0 \quad \frac{\partial \zeta}{\partial t} = \frac{k}{\mu}\nabla^2 p \tag{1}$$

$$\dot{\zeta} = \alpha \dot{\varepsilon}_{ii} + Q'\dot{p} - \gamma_2 \dot{T} \tag{2}$$

$$\dot{T}_f + \nabla(J_f T_f) - c_f{}^T \nabla^2 T_f = 0 \tag{3}$$

$$\dot{T}_R - c_R{}^T \nabla^2 T_R = 0 \tag{4}$$

Where, K is the bulk modulus , G is the shear modulus , u is the displacement, α is the Biot's coefficient, γ_1 is the thermal expansion coefficient of solid, γ_2 is the thermal expansion coefficient of fluid (K^{-1}), T_R is the rock temperature, T_f is the fluid temperatures and p is the pore pressure. The above governing equations have allowed us to formulate instantaneous non-equilibrium heat transfer between fluid in fracture and matrix which results in stress perturbation. In instantaneous non-equilibrium, the solid matrix has a different temperature from that of the saturating fluid and the temperature difference between two phases decreases with time until it reaches a state at which it may be considered as instantaneous equilibrium. A schematic of the model setup for instantaneous non-equilibrium is shown in Fig. 4.
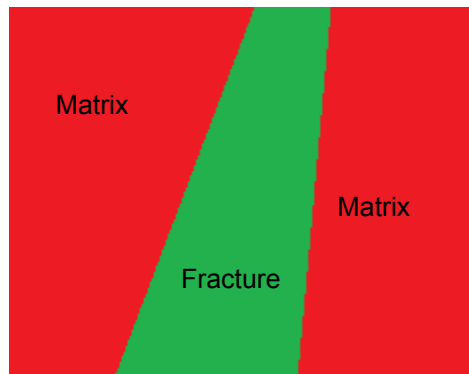

Figure 4: *Fracture cutting through the matrix*

In instantaneous non-equilibrium heat transfer within the rock is modelled by conduction and heat transfer in fluid by conduction and convection. The system of linear equations is solved by Staggered Partitioning method and the Predictor-corrector steps used to obtain stable temperature results.

Fracture Response to Stimulation model

The analytical model recently developed by Kotousov and Rahman, et al 2011 is used to model the shear slippage of the fracture surfaces with respect to each other which causes a change in the

fracture aperture. Two main assumptions are made for this purpose. Firstly, the sliding of the fracture surfaces with respect to each other which is characterized by the classical Coulomb friction law as:

$$\tau_n = \tau_0 + f\sigma_n \tag{5}$$

Where, τ_0 is the threshold shear stress at which the fracture surfaces start to slide, f is the friction factor, σ_n is the normal stress and τ_n is the shear stress during the slippage.

Next, the fracture aperture is described based on the surrounding in-situ stress condition. In this model any shear displacement of fracture surfaces causes the fracture to open. The effect of surface roughness is simulated by distributed elastic springs as illustrated in Fig.5.
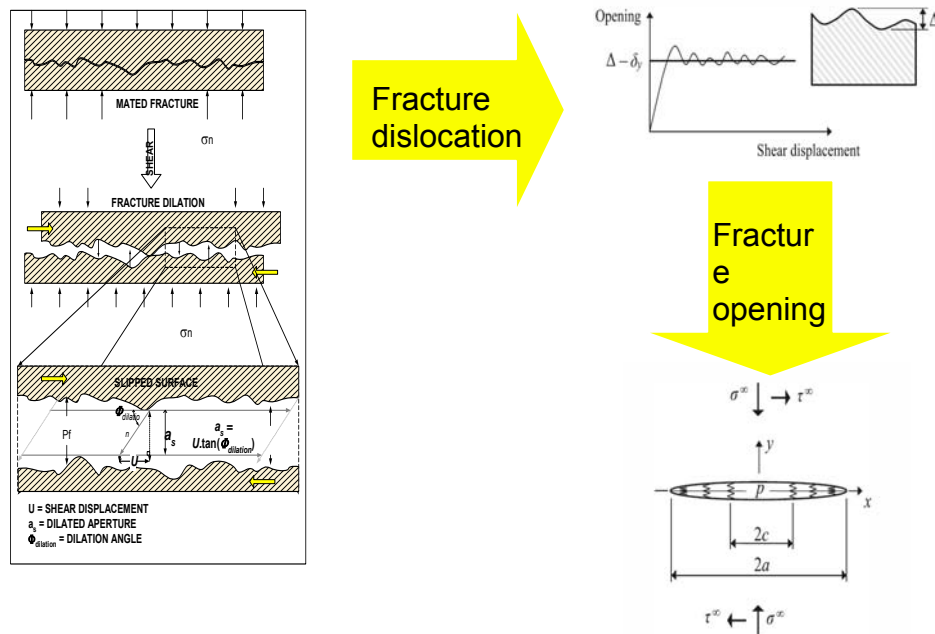

Figure 5: Roughness induced opening of fractures are modeled using distributed dislocation densities.

The contact between surfaces diminishes when the opening exceeds the overall the roughness of the fracture surfaces. The constitutive equations for the adopted simplified model are as follow:

$$\sigma_n = k\overline{E}(\Delta - \delta_y) \quad \delta_y < \Delta \tag{6}$$

$$\sigma_n = 0 \quad \delta_y \geq \Delta \tag{7}$$

Δ is the characteristic height of the fracture. Also E is the Young modulus of elasticity and k is the spring constant. The above set equations are solved numerically using dislocation density to obtain values for fracture opening due to induced fluid pressure.

Results and Discussion

Initially, field data, such as the reservoir structure, fracture orientation, size and other fracture parameters from Patchawarra geothermal reservoir, which influence reservoir performance, are acquired from the open literature.

This information is used to investigate fracture stimulation by injected fluid pressure and thermal stress and consequent changes in permeability (in terms of Log_{10} RMS fluid velocity) both in short and long term. The reservoir permeability for each block is calculated based on the discrete fracture network data and fluid flow simulation. Then the pore pressure, Log_{10} RMS velocity, temperature and stress tensor across the reservoir for a given induced fluid pressure at each time step are estimated. The residual fracture aperture as a result of change in local effective stress are determined and evaluated.

The reservoir is pressurized by injecting fluid through the injection well. To increase the injectivity, a pair of co-planar fractures of half-length of 50m is placed at both the injection and production wells. The pressurization was carried out over a period of 60 weeks. During the pressurization, the change in fracture width for each individual natural fracture and the resulting permeability tensor were calculated. Following stimulation of the reservoir, a flow test was carried out over a period of 20 years. During the flow test, changes in fracture apertures due to thermo-poro-elastic stresses and the consequent changes in permeability were determined. Also estimated were the thermal drawdown, produced fluid temperature and production rate.

Effect of stimulation time on shear dilation

Results of shear dilation are presented as average percentage increase in fracture aperture and dilation events with time (see Figs.6 and 7a, b and c). From Fig. 6, it can be seen that there exists three distinct aperture histories: 0-40 weeks, 40-50 weeks and 50 weeks and above. Until about 40 weeks, there exists a slow but linear increase in occurrence of dilation events due to induced fluid pressure of 51.7 MPa (bottomhole) and the average increase in aperture reaches a value of about 18%. Following this, the rate of occurrence of dilation events increases sharply until about 50 weeks thus, reaching 60% average increase in fracture aperture. After this time, no significant dilation events can be observed (a plateau of events is reached). This infers that for every set of reservoir and stress parameters as well as injection schedule, an optimum level of shear dilation can be achieved. In Figs. 7 (a, b and c) the dilation events at different stimulation times are presented. From these figures it can be seen that it takes about 50 weeks for shear dilation events to reach the production well. When the results of this study are compared with previous study (Koh and Rahman et al, 2011), in which shear dilation events are estimated based on a simplistic model Willis-Richards et al, 1996) a number of differences can be observed. Firstly the time required to overcome the threshold stress is 40 weeks which is about 12 weeks longer than the previous studies. Secondly, the time required to create maximum effective reservoir volume is almost 20 weeks longer than that the previous studies (40 weeks). Thus results of this study clearly demonstrate that the material properties, such as the surface roughness and Modulus of Elasticity used to estimate residual aperture provide a more conservative prediction of shear displacement events and the resulting residual aperture. These results also show that the reservoir volume (interconnected fracture networks for effective the heat transfer area) estimated by the new stimulation technique (this study) is much smaller (lower retained fracture aperture) which is in consistent with experiences with most EGS trials.
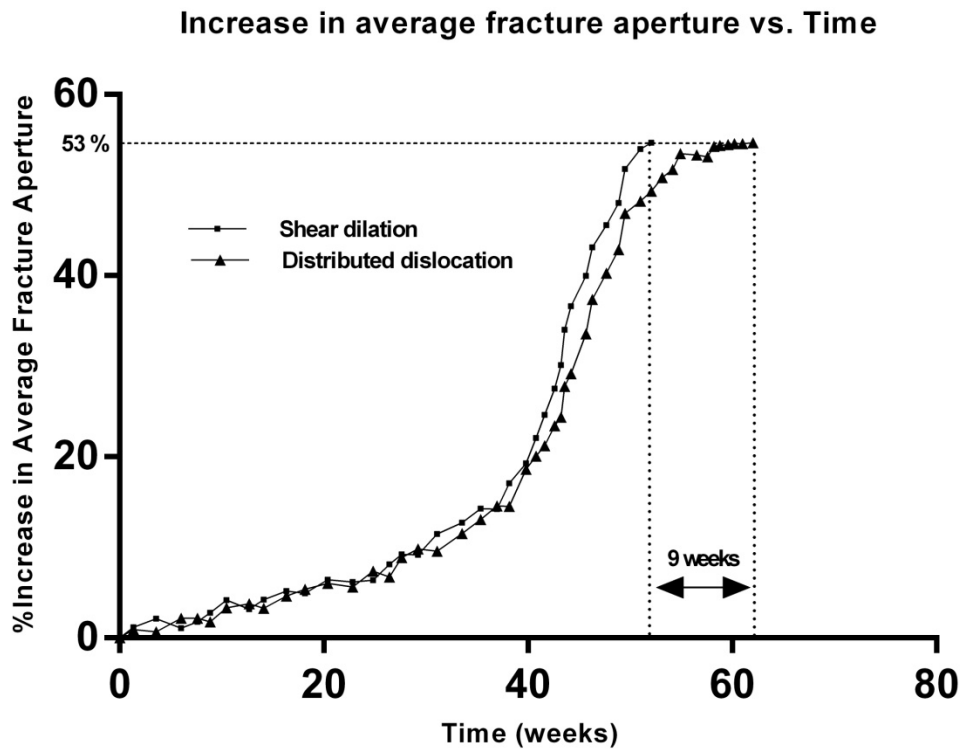
Increase in average fracture aperture vs. Time

Fig. 5: *Increase in average fracture aperture (retainable) with stimulation time. Strike slip stress regime with σH = 78.9 MPa and σh = 53.3 MPa, P_{inj} = 68.9 MPa,*
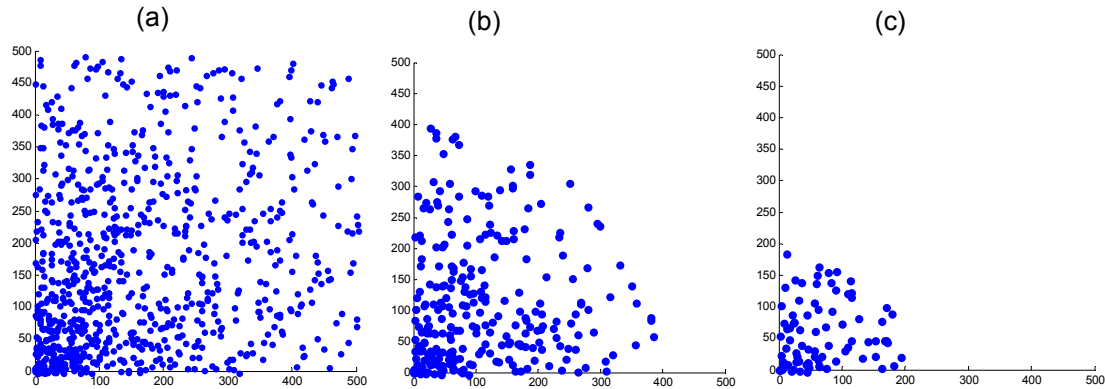

Fig. 6: *Cumulative shear dilation events of the fracture network during different stages of stimulation: after (a) 1 week, (b) after 24 weeks and (c) after 52 weeks for a strike slip stress regime with σH = 78.9 MPa and σh = 44.8 MPa, P_{inj} = 51.7 MPa. The event's locations are in the Cartesian coordinates in meters.*

Numerical flow test

Following the 60 weeks of stimulation, a flow test was carried out with a bottomhole injection pressure of 32.6 MPa and a production pressure of 22.3 MPa (at a reservoir impedance of 10 MPa between the injection and production wells) for period of 20 years. During this production period, pore pressure profile, Log_{10} root means square (RMS) velocity profile (which is directly proportional to the permeability), effective stress and the matrix temperature drawdown are monitored. In Figs 7 (a, b, and c) and 8 (a, b, and c) the Log_{10} RMS fluid velocity profile and the pore pressure after 1 year, 10 years and 20 years are presented respectively. From the results this study it can be observed that during the early production period (one month) high pore pressure is primarily built up around the injection well and the flow of fluid is primarily through major inter-connected flow paths (see Figs 7 a

and 8 a). With the progress of time the injection pressure advances towards the production well and at the about 10 years of production time it reaches half way between the injection and production wells. By this time the fluid sweeps through a significant part of the reservoir. During 20 years of production produced fluid temperature dropped from 200 to 140 °C (see Fig.11). Because of the low fluid contact area at the early stage of production, the heat transfer and the resulting thermal drawdown is very low. With the pass of time the fluid sweeps over a large part of the reservoir which increases thermal drawdown. At the end of the 20 years of production the average matrix temperature drops from 200 to 150°C which is quite low (drop) compared to previous study (Koh and Rahman, 2011). This is due to the fact that previous study is based in thermal equilibrium.
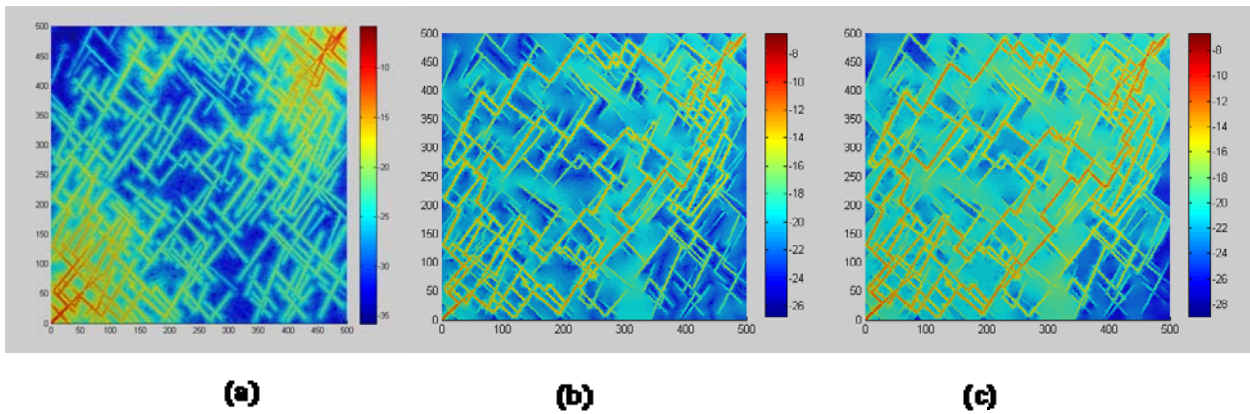

(a) **(b)** **(c)**

Figure 7: *Log10 RMS fluid velocity profile of the Patchawarra reservoir (a) after 1 year, (b)after 10 years and (c) after 20 years of production with σH = 78.9 MPa and σh = 44.8 MPa, P$_{inj}$ = 32.6 MPa.*
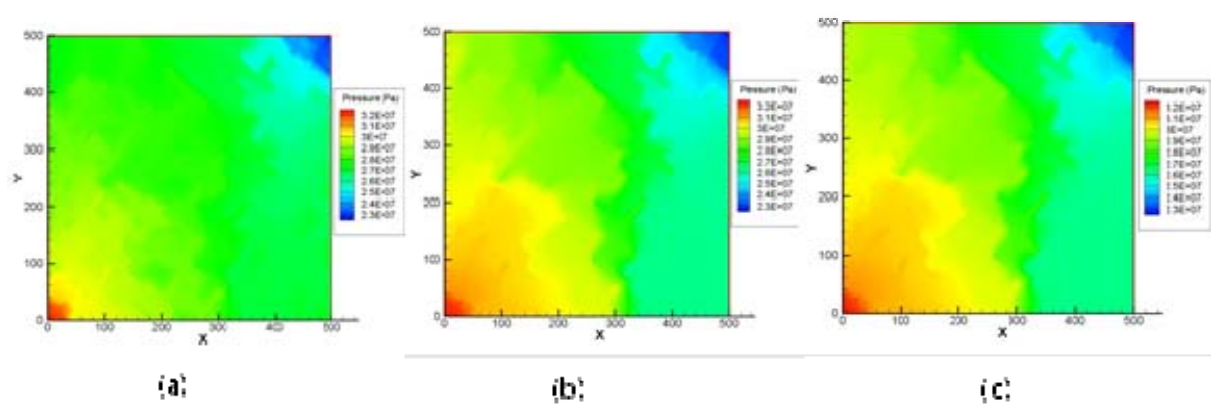

Figure 8: *Pore pressure of the Patchawarra reservoir (a) after 1 year, (b) after 10 years and (c) after 20 years of production with σH = 78.9 MPa and σh = 44.8 MPa, P$_{inj}$ = 32.6 MPa.*

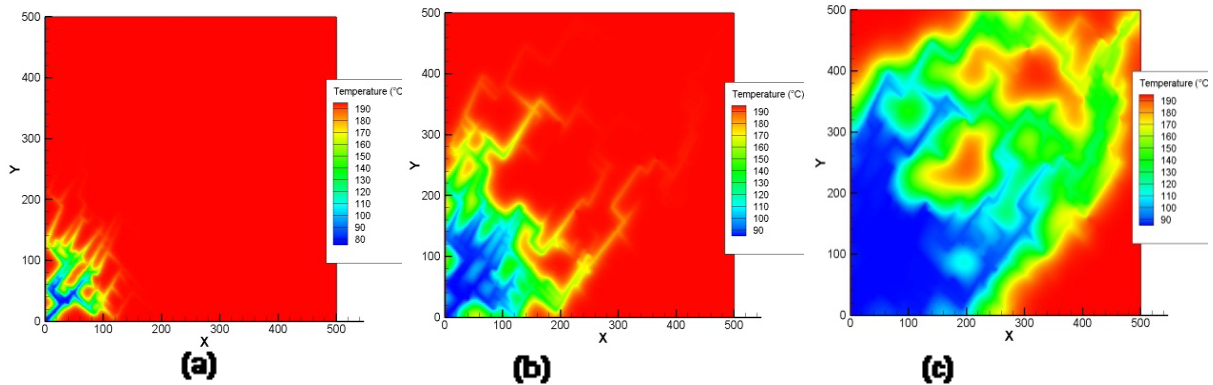**Figure 9:** *Matrix temperature of the Patchawarra reservoir after a)1, b)10 and c)20 years of production with σH = 78.9 MPa and σh = 44.8 MPa, Pinj = 32.6 MPa.*

In Fig.10 the x- and y components of effective stress distribution of the Patchawarra geothermal reservoir during different stages of production are presented. These results show that by the end of 20 years of production the effective stresses throughout the reservoir are significantly reduced, thus allowing most fractures to open and conduct fluid. The reduction in the effective stresses is caused by the circulating fluid as well as thermal drawdown. Also the effect of local thermal non-equilibrium is presented in Fig.10 which shows that there is a significant difference in the produced fluid temperature with and without the local thermal equilibrium.
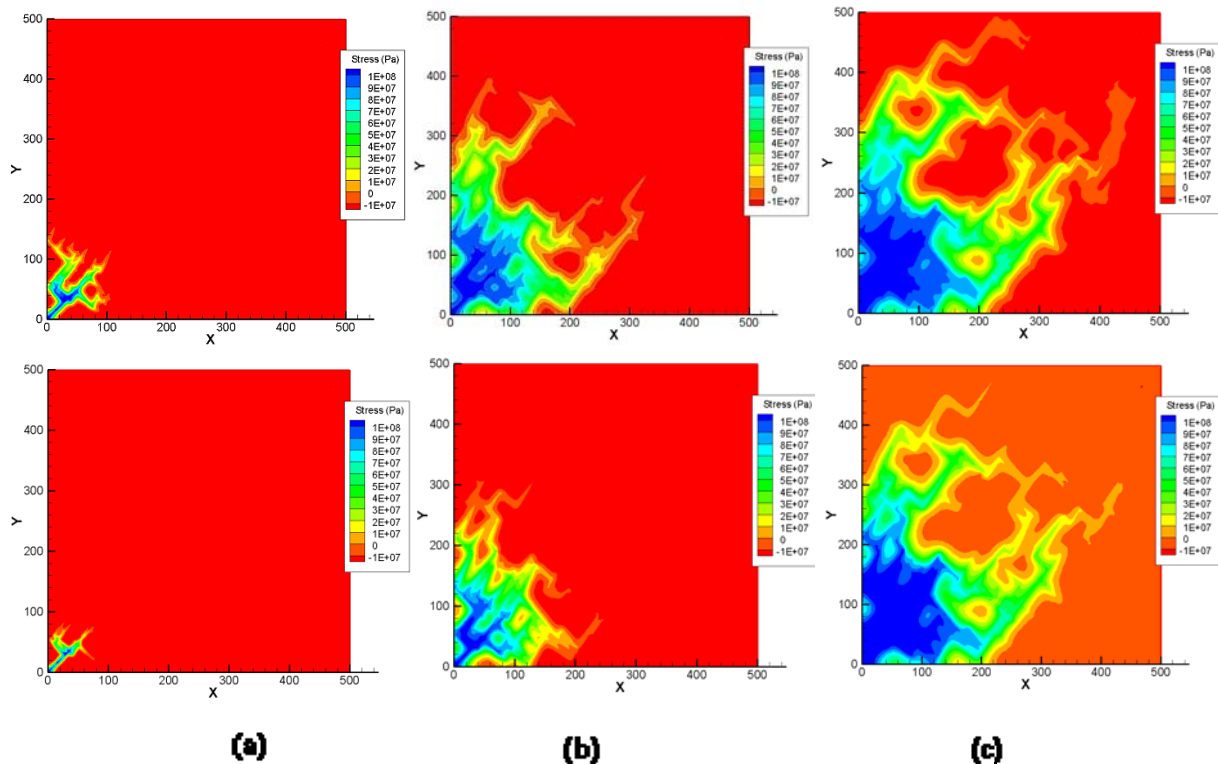

Figure 10: *x (top) and y (bottom) components of effective stress distribution at different production stages: (a) after 1 year, (b) after 10 years and (c) after 20 years for σH = 78.9 MPa and σh = 44.8 MPa, Pinj = 32.6 MPa and Pprod=22.3 MPa, Tinj = 80 °C, Tmatr = 200 °C*
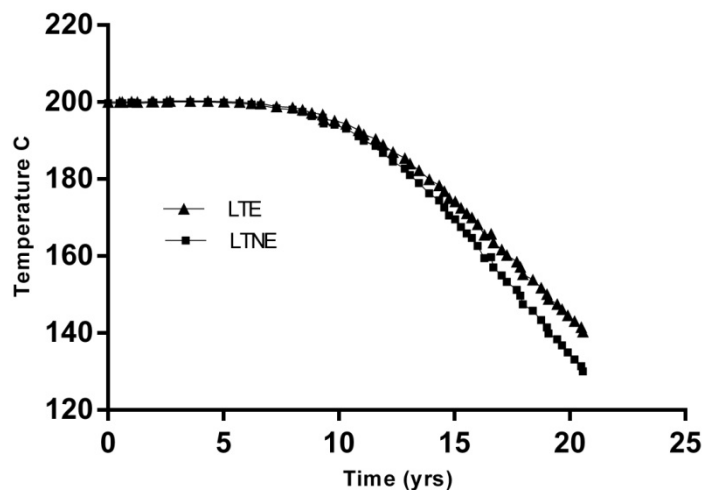
Figure 11: *Matrix temperature drawdown as a function time: a comparison between local thermal equilibrium (LTE) and local thermal non-equilibrium (LTNE).*

Conclusions

1. The hybrid of numerical simulation of tectonic history and stochastic analysis of field data provides a more realistic generation of subsurface discrete fracture map.

2. A fully coupled thermo-poro;elastic reservoi model has allowed us to study changes in stresses and resulting permeability of the reservoir.

3. Formulation of local thermal non-equilibrium has also allowed us to estimate stress gradient between fracture and matrix due to circulating fluid.

4. The new technique of simulating shear dilation using dislocation densities provides a more realistic assessment of reservoir stimulation by induced fluid pressure and temperature drawdown by circulating fluid.

References

Baria, R., Baumg¨artner, J., G´erard, A., Jung, R., Garnish, J., 1999. European HDR research programme at Soultz-sous-Forˆets (France) 1987–1996. Geothermics 28, 655–669.

Beeler, N.M., Simpson, R.W., Hickman, S.H. and Lockner, D.A., 2000. Pore fluid pressure, apparent friction, and Coulomb failure, J. Geophys. Res. 105, 25533– 25542.

Beeler, N. M., Wong, T. F. & Hickman, S. H., 2003. On the expected relationships among apparent stress, static stress drop, effective shear fracture energy, and efficiency. Bull. Seismol. Soc.Am. 93, 1381-1389.

Ghassemi, A. and G. Suresh Kumar (2007). "Changes in fracture aperture and fluid pressure due to thermal stress and silica dissolution/precipitation induced by heat extraction from subsurface rocks." Geothermics 36(2): 115-140.

Ghassemi, A., Nygren, A., Cheng, A., 2008. Effects of heat extraction on fracture aperture:A poro–thermoelastic analysis. Geothermics 37, 525–539.

Gentier, S., Rachez, X., Ngoc, T. D. T., Peter-Borie, M. and Souque, C. (2010). "3D Flow Modelling of the Medium-Term Circulation Test Performed in the Deep Geothermal Site of Soultz-Sous-forets (France). Proceedings Worlf Geothermal Congress 2010 - Bali, Indonesia, 25-29 April 2010.

Jing, Z., J. Willis-Richards, et al. (2000). "A three-dimensional stochastic rock mechanics model of engineered geothermal systems in fractured crystalline rock." J. Geophys. Res. 105.

Koh, J., H. Roshan, et al. (2011). "A numerical study on the long term thermo-poroelastic effects of cold water injection into naturally fractured geothermal reservoirs." Computers and Geotechnics 38(5): 669-682.

Kumar, G.S. and Ghassemi, A., 2005. Numerical modeling of non-isothermal quartz dissolution/precipitation in a coupled fracture–matrix system. Geothermics 34 (2005) 411–439.

McDermott, C.I. and Kolditz, O., 2006. Geomechanical model for fracture deformation under hydraulic, mechanical and thermal loads. Hydrogeol. J. 14, 487–498.

Mildren, S., J. Burgess, et al. (2005). Multiple Application of Image Log Data to EOR Operations in the Cooper Basin, Australia. SPE International Improved Oil Recovery Conference in Asia Pacific. 5-6 December, Kuala Lumpur, Malaysia.

Murphy, P. Negraru and M. Richards 2007 Impact of enhanced geothermal systems on US energy supply in the twenty-first century Journal: Philosophical Transactions of the Royal Society A: Mathematical, Physical and Engineering Sciences Volume: 365 Issue: 1853 Pages: 1057-1094 Date: April 15, 2007

Muskat, M. (1937). The Flow of Homogeneous Fluids Through Porous Media, Edwards Publisher.

Narayan, S. P., Z. Yang, et al. (1998). HDR reservoir development by fluid induced shear dilation: A numerical study of the Soultz and the Cooper Basin granite rock. International Hot Dry Rock - Forum, Strasbourg, France.

O'Sullivan, M.J., Pruess, K., Lippmann, M.J., 2001. Geothermal reservoir simulation. The state of practice and emerging trends. Geothermics 30 (4), 395–429.

Rahman, M. K., M. M. Hossain, et al. (2000). "An analytical method for mixed-mode propagation of pressurized fractures in remotely compressed rocks." International Journal of Fracture 103(3): 243-258.

Rahman, M. K., M. M. Hossain, et al. (2002). "A Shear-Dilation-Based Model for Evaluation of Hydraulically Stimulated Naturally Fractured Reservoirs." Int. J. for Numerical and Analytical Methods in Geomech. 26(5).

Sanyal, S. K., E. E. Granados, et al. (2005). An Alternative and Modular Approach to Enhanced Geothermal Systems. World Geothermal Congress 2005, Antalya, Turkey.

Sausse, J., Desayes, C. and Genter, A. (2007). "From geological interpretation and 3D modelling to the characterization of the deep seated EGS reservoir of Soultz (France)." Proceedings European Geothermal Congress 2007, Unterhaching, Germany, May 30-June 1, 2007.

Shaik, A. R., M. A. Aghighi, et al. (2008). "An Innovative reservoir simulator can Help Evaluate Hot Water Production for Economic Development of Australian Geothermal reservoirs." GRC Transactions 32: 97 102.

Shaik, A.R., Koh, J., Rahman, S. S., Aghighi, M. A. and Tran, N. H., 2009. Design and evaluation of well placement and hydraulic stimulation for economical heat recovery from enhanced geothermal systems. GRC Annual Meeting October 4–7, 2009, conference proceedings.

Shaik, A. R., S. S. Rahman, et al. (2011). "Numerical simulation of Fluid-Rock coupling heat transfer in naturally fractured geothermal system." Applied Thermal Engineering 31(10): 1600-1606.

Shaik, A.R., Koh, J., Rahman, S. S., Aghighi, M. A. and Tran, N. H., 2009. Design and evaluation of well placement and hydraulic stimulation for economical heat recovery from enhanced geothermal systems. systems. GRC Annual Meeting October 4–7, 2009, conference proceedings.

Tran, N., Z. Chen, et al. (2007). "Characterizing and modelling of fractured reservoirs with object-oriented global optimization." Journal of Canadian Petroleum Technology 46(3): 39-45.

J. W. Tester, B. J. Anderson, A. S. Batchelor, D. D. Blackwell, R. DiPippo, E. M. Drake, J. Garnish, B. Livesay, M. C. Moore, K. Nichols, S. Petty, M. Nafi Toksoz, R. W. Veatch, R. Baria, C. Augustine, E.

Willis-Richards, J., K. Watanabe, et al. (1996). "Progress toward a stochastic rock mechanics model of engineered geothermal systems." J. Geophys. Res. 101(B8): 17481-17496.

Zimmermann, G., Moeck, I., Blöcher, G. (2010): Cyclic waterfrac stimulation to develop an enhanced geothermal system (EGS): Conceptual design and experimental results. - Geothermics, 39, 1, 59-69

Zhou, X. X., Ghassemi, A. and Cheng, A. H.-D., 2009. A three-dimensional integral equation model for calculating poro- and thermoelastic stresses induced by cold water injection into a geothermal reservoir. Int. J. Numer. Anal. Meth. Geomech. 2009; 33,1613–1640